DESY 06-062, RCNP-Th 06004, MKPH-T-06-12

Nonperturbative determination of the QCD potential at $O(1/m)$

Yoshiaki Koma[a], Miho Koma[a,b], Hartmut Wittig[c]

[a] *Deutsches Elektronen-Synchrotron DESY, Theory Group, D-22607 Hamburg, Germany*

[b] *Research Center for Nuclear Physics (RCNP), Osaka University, Osaka 576-0047, Japan*

[c] *Institut für Kernphysik, Johannes Gutenberg-Universität Mainz, D-55099 Mainz, Germany*

The relativistic correction to the QCD static inter-quark potential at $O(1/m)$ is investigated nonperturbatively for the first time by using lattice Monte Carlo QCD simulations. The correction is found to be comparable with the Coulombic term of the static potential when applied to charmonium, and amounts to one-fourth of the Coulombic term for bottomonium.

PACS numbers: 11.15.Ha, 12.38.Gc, 12.39.Pn

I. INTRODUCTION

Heavy quarkonia, i.e. bound states of a heavy quark and antiquark [1, 2, 3, 4], offer a unique opportunity to gain an understanding of nonperturbative QCD. A possible way of studying such systems systematically in QCD is to employ nonrelativistic QCD (NRQCD) [5, 6], which is obtained by integrating out the scale above the heavy quark mass $m \gg \Lambda_{\rm QCD}$. Further, by integrating out the scale mv, where v is quark velocity, one arrives at a framework called potential NRQCD (pNRQCD) [7, 8, 9, 10], where the static potential emerges as the leading-order contribution, followed by relativistic corrections in powers of $1/m$. The potential at $O(1/m^2)$ contains the leading order spin-dependent corrections [11, 12, 13] and the velocity-dependent potentials [14, 15]. Perturbation theory may be applied to the determination of these potentials to some extent. However, since the binding energy is typically of the scale mv^2, which can be of the same order as $\Lambda_{\rm QCD}$ due to the nonrelativistic nature of the system, $v \ll 1$, as well as the fact that perturbation theory cannot incorporate quark confinement, it is essential to determine the potential nonperturbatively. The various properties of heavy quarkonium can be extracted by solving the Schrödinger equation with these potentials.

Monte Carlo simulations of lattice QCD offer a powerful tool for the nonperturbative determination of the potentials, and it is the aim of this Letter to present the simulation result of the heavy quark potential at $O(1/m)$, which has not been investigated so far on the lattice. Let us denote the spatial position of the quark and antiquark as $\vec{r}_1$ and $\vec{r}_2$ with the relative distance $r = |\vec{r}_1 - \vec{r}_2|$ and the masses m_1 and m_2, respectively. The potential is

$$V(r) = V^{(0)}(r) + \left(\frac{1}{m_1} + \frac{1}{m_2}\right) V^{(1)}(r) + O(\frac{1}{m^2}) \ , \quad (1)$$

where $V^{(0)}(r)$ is the static potential, usually obtained by evaluating the expectation value of the Wilson loop. The static potential is well parameterized by the Coulomb plus linear term,

$$V^{(0)}(r) = -\frac{c}{r} + \sigma r + \mu \ , \quad (2)$$

where σ is the string tension and μ a constant [29]. On the other hand, the nonperturbatively expected form of $V^{(1)}(r)$ is not yet known, but leading-order perturbation theory yields $V^{(1)}(r) = -C_F C_A \alpha_s^2/(4r^2)$ [8, 16, 17], where $C_F = 4/3$ and $C_A = 3$ are the Casimir charges of the fundamental and adjoint representations, respectively (beyond leading-order perturbation theory, see [18]).

II. PROCEDURES

We work in Euclidean space in four dimensions on a hypercubic lattice with lattice volume $V = L^3T$ and lattice spacing a, where periodic boundary conditions are imposed in all directions. Writing the eigenstate of the pNRQCD Hamiltonian at $O(m^0)$ in the $\mathbf{3} \otimes \mathbf{3}^*$ representation of color SU(3), which corresponds to the static quark-antiquark state, as $|n\rangle \equiv |n; \vec{r}_1, \vec{r}_2\rangle$ with the energy $E_n(r)$ [e.g., $E_0(r) = V^{(0)}(r)$], the spectral representation of $V^{(1)}(r)$ is expressed as [8, 9]

$$V^{(1)}(r) = -\frac{1}{2} \sum_{n=1}^{\infty} \frac{\langle 0|g\boldsymbol{E}(\vec{r}_i)|n\rangle \cdot \langle n|g\boldsymbol{E}(\vec{r}_i)|0\rangle}{(\Delta E_{n0})^2} \ , \quad (3)$$

where g is the gauge coupling, $\boldsymbol{E}(\vec{r}_i)$ denotes the electric field attached to the quark ($i = 1$) or the antiquark ($i = 2$), and $\Delta E_{n0} \equiv E_n - E_0$ the energy gap. It is also possible to write Eq. (3) as the integral of the electric field strength correlator on the Wilson loop with respect to the relative temporal distance between two electric fields [8, 9]. This is, in principle, measurable on the lattice, and the result is reduced to Eq. (3) once the spectral decomposition is applied by using the transfer matrix theory, and the temporal size of the Wilson loop is taken to infinity [30].

In our approach, the Polyakov loop correlation function (PLCF, a pair of Polyakov loops P separated by a

distance r) is adopted as the quark-antiquark source instead of the Wilson loop for the reason discussed below. Let us consider the field strength correlator on the PLCF,

$$C(t) = \langle\!\langle g^2 \boldsymbol{E}(\vec{r}_i, t_1)\cdot\boldsymbol{E}(\vec{r}_i, t_2)\rangle\!\rangle_c \equiv \langle\!\langle g^2 \boldsymbol{E}(\vec{r}_i, t_1)\cdot\boldsymbol{E}(\vec{r}_i, t_2)\rangle\!\rangle - \langle\!\langle g\boldsymbol{E}(\vec{r}_i)\rangle\!\rangle\cdot\langle\!\langle g\boldsymbol{E}(\vec{r}_i)\rangle\!\rangle \ , \quad (4)$$

where the double brackets represent the ratio of expectation value $\langle\!\langle\cdots\rangle\!\rangle = \langle\cdots\rangle_{PP^*}/\langle PP^*\rangle$, while $\langle\cdots\rangle_{PP^*}$ implies that the electric field is connected to either of the Polyakov loop in a gauge invariant way. The relative temporal distance of two electric field operators is $t = t_2 - t_1$.

The spectral decomposition of Eq. (4) reads [19]

$$C(t) \ = \ 2\sum_{n=1}^{\infty}\langle 0|g\boldsymbol{E}(\vec{r}_i)|n\rangle\cdot\langle n|g\boldsymbol{E}(\vec{r}_i)|0\rangle e^{-(\Delta E_{n0})T/2} \times\cosh[(\Delta E_{n0})(T/2-t)]+O(e^{-(\Delta E_{10})T}) \ , \quad (5)$$

where the last term represents terms involving exponential factors equal to or smaller than $\exp[-(\Delta E_{10})T]$. Thus, once Eq. (4) is evaluated via Monte Carlo simulations, we can determine the amplitude $|\langle 0|g\boldsymbol{E}(\vec{r}_i)|n\rangle|^2$ and the energy gap ΔE_{n0} in Eq. (5) by a fit and insert them into Eq. (3). It is easy to see that in the limit $T\to\infty$ we can write Eq. (4) in the integral form $V^{(1)}(r) = -(1/2)\lim_{\tau\to\infty}\int_0^\tau dt\ tC(t)$, where $\tau = \eta T$ with arbitrary $\eta\in(0, T/2]$.

The reason for using the PLCF is to compute Eq. (3) with less systematic errors. The hyperbolic cosine in Eq. (5) is typical for the PLCF and we can control the effect of the finite temporal lattice size on the field strength correlator automatically in the fit. Moreover, the error term of $O(e^{-(\Delta E_{10})T})$ is already expected to be small for a reasonable size of T. By contrast, if one uses the Wilson loop at this point, the spectral representation is just a multi-exponential function, and the leading error term is of $O(e^{-(\Delta E_{10})(\Delta t)})$, where Δt is the relative temporal distance between the spatial part of the Wilson loop and the field strength operator. Here, one cannot choose Δt as large as T, since the temporal extent of the Wilson loop is limited to $T/2$ because of the periodicity of the lattice volume.

The only technical problem that arises when using the PLCF is how to obtain a signal for the field strength correlator in Eq. (4), since the expectation value of the PLCF at zero temperature becomes exponentially small with increasing r, and the signal is easily washed out by statistical noise. In fact, it is almost impossible to obtain the signal of the PLCF at intermediate distances, say $r\approx 0.5$ fm, with the commonly used simulation algorithms. However, we find that this problem can be solved by applying the multi-level algorithm [20] with a certain modification as applied to the determination of the spin-dependent potentials [19, 21] (see also [22] for a similar application).

The basic procedure of the multi-level algorithm (restricted to the lowest level) is as follows. We first divide the lattice volume into several sublattices along the time direction, where a sublattice consists of a certain number of time slices $N_{\rm tsl}$. The number of sublattices is $N_{\rm sub} = T/N_{\rm tsl}$, which is assumed to be integer. In each sublattice we take averages of the components of the correlation function [components of the PLCF and of the field strength correlators, which are in the $\mathbf{3}\otimes\mathbf{3}^*$ representation of SU(3)], by updating the gauge field with a mixture of heatbath (HB) and over-relaxation (OR) steps, while the spatial links on the boundary between sublattices remain intact during the update. We refer to this procedure as the internal update and denote the number of internal update as $N_{\rm iupd}$. Repeating the internal update until we obtain stable signals for these components, we finally multiply these averaged components to complete the correlation function. Thereby the correlation function is obtained for one configuration. For a schematic understanding, see Fig. 1, which illustrates the computation of the electric field strength correlator on the PLCF. We then update the whole set of links without specifying any layers to obtain another independent gauge configuration and repeat the above sublattice averaging. Once $N_{\rm tsl}$ and $N_{\rm iupd}$ are optimized for a given gauge coupling β and a maximal quark-antiquark distance of interest, the statistical fluctuations of observables turn out to be quite small. Further technical details can be found in [19].

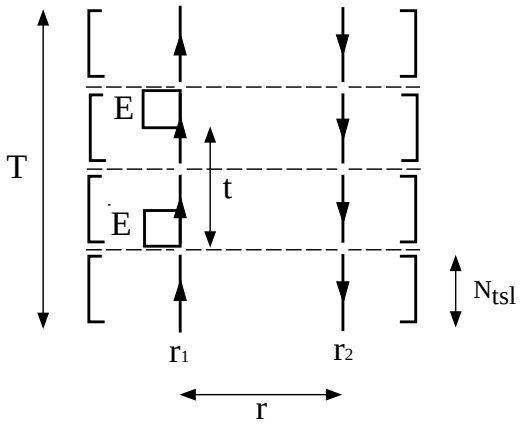

FIG. 1: Construction of the electric field strength correlator on the PLCF. Arrows at $\vec{r}_1$ and $\vec{r}_2$ represent the Polyakov lines for the static quark and antiquark. $[\cdots]$ denotes the sublattice average.

III. RESULTS

Our simulations were carried out using the standard Wilson gauge action in SU(3) lattice gauge theory at $\beta = 6.0$ on the 20^4 lattice (the lattice spacing, determined from the Sommer scale $r_0 = 0.5$ fm, is $a\approx 0.093$ fm [20]). One Monte Carlo update consisted of 1 HB, followed by 5 OR steps. For practical reasons (mainly to save computer memory) we set $\vec{r} = (r, 0, 0)$. We employed the lattice field strength operator defined by $ga^2F_{\mu\nu}(s) \equiv [U_{\mu\nu}(s) - U^\dagger_{\mu\nu}(s)]/(2i)$ at the site s, where $U_{\mu\nu}(s)$ are

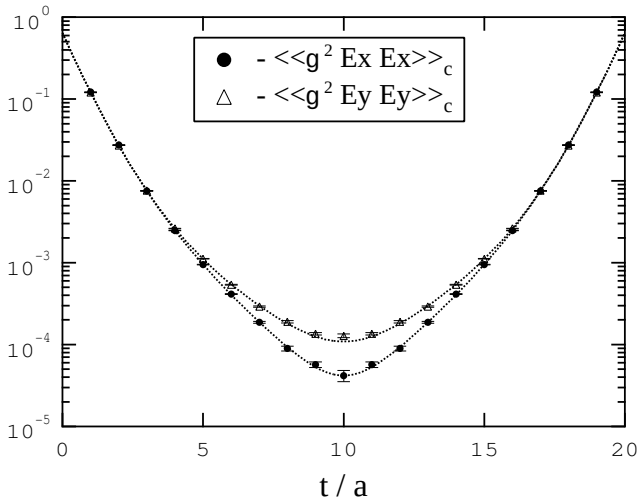

FIG. 2: The electric field strength correlators on the PLCF at $\beta = 6.0$ on the 20^4 lattice for $r/a = 5$. The dotted lines are the fit curves with $n_{\max} = 3$ in Eq. (5).

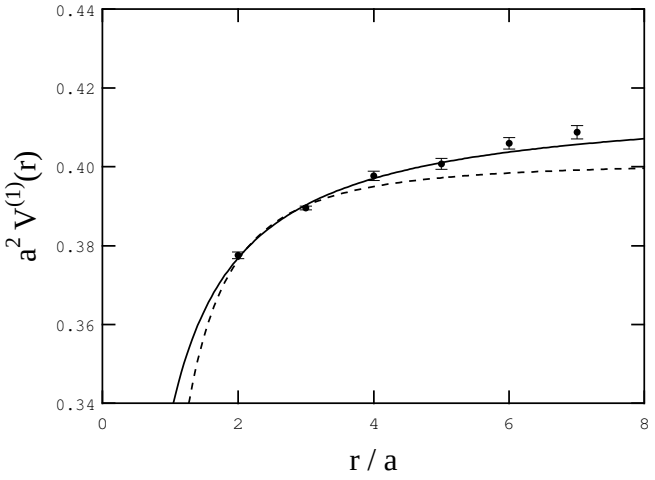

FIG. 3: The potential at $O(1/m)$, $V^{(1)}(r)$. Dashed and solid lines are the fit curves corresponding to Eq. (6) and Eq. (7), respectively.

plaquette variables and constructed the electric field by $ga^2E_i(s) = ga^2[F_{4i}(s) + F_{4i}(s - \hat{i})]/2$. In order to remove self-energy contributions of the electric field we multiplied by the conventional Huntley-Michael factor, $Z_{E_i}(r)$ [23], which, however, only removes self-energy contributions at $O(g^2)$. This factor, which depends on r and also on the relative orientation of the electric field operator to $\vec{r}$, was computed using the PLCF [19]. We obtained the value $Z_{E_i}(r) \approx 1.62$. For a more precise value of Z_E, see Ref. [19]. For the chosen value of $N_{\rm tsl} = 4$ we performed $N_{\rm iupd} = 7000$ internal updates. Our total statistics was $N_{\rm conf} = 60$.

In Fig. 2, we show the $C(t)$ for the longitudinal and the transverse components, $\langle\!\langle g^2 E_x(\vec{r}_i, t_1) E_x(\vec{r}_i, t_2)\rangle\!\rangle_c$ and $\langle\!\langle g^2 E_y(\vec{r}_i, t_1) E_y(\vec{r}_i, t_2)\rangle\!\rangle_c = \langle\!\langle g^2 E_z(\vec{r}_i, t_1) E_z(\vec{r}_i, t_2)\rangle\!\rangle_c$, respectively, where $r/a = 5$ is selected as an example. Note that the correlators are negative. Here, the second term of Eq. (4) can be non-zero as the electric field is even under CP transformations. We computed $\langle\!\langle gE_i\rangle\!\rangle$ independently and found $\langle\!\langle gE_y\rangle\!\rangle = \langle\!\langle gE_z\rangle\!\rangle = 0$, while $\langle\!\langle gE_x\rangle\!\rangle \neq 0$, which was then subtracted to obtain $C(t)$. As it is impossible to determine the amplitudes and the energy gaps for all $n \geq 1$ with the limited data points, we truncated the expansion in Eq. (5) at a certain $n = n_{\max}$. The validity of the truncation was monitored by looking at χ^2 and the stability of the resulting potential as a function of $n_{\max}$, where χ^2 was always defined with the full covariance matrix. We found that $n_{\max} = 3$ was optimal with the fit range $t/a \in [1, 8]$ (equivalent to $t/a \in [12, 19]$). The systematic effect caused by the truncation can be checked by simulating volumes with larger values of T and by increasing $n_{\max}$ in the fit. However, from the experience of evaluating similar field strength correlators for the spin-dependent potentials [19], we expect that such an effect is already negligible compared to statistical errors, once three terms are included for $T = 20$ at $\beta = 6.0$. Here, we employed two ways of the fit procedure; we fitted $\langle\!\langle g^2 E_x E_x\rangle\!\rangle_c$ and $\langle\!\langle g^2 E_y E_y\rangle\!\rangle_c$ separately, and fitted $\langle\!\langle g^2 \boldsymbol{E}\cdot\boldsymbol{E}\rangle\!\rangle_c = \langle\!\langle g^2 E_x E_x\rangle\!\rangle_c + 2\langle\!\langle g^2 E_y E_y\rangle\!\rangle_c$ simultaneously. The latter is based on the expectation that the energy gaps are the same for both correlators. We obtained $\chi^2_{\rm min}/N_{\rm df} = 1.1$ for $\langle\!\langle g^2 E_x E_x\rangle\!\rangle_c$ and 3.0 for $\langle\!\langle g^2 E_y E_y\rangle\!\rangle_c$, respectively, and the corresponding fit curves are plotted in Fig. 2. $N_{\rm df}$ is the number of degrees of freedom. The simultaneous fit yielded $\chi^2_{\rm min}/N_{\rm df} = 2.2$. In any case, the resulting potential was found to be the same within errors, which were estimated from the distribution of the jackknife sample of the fit parameters. For other distances $\chi^2_{\rm min}/N_{\rm df}$ was smaller than in this example, and the results of the two fit procedures were consistent.

We present the potential $V^{(1)}(r)$ in Fig. 3, where the result of the simultaneous fit is plotted. We see an increasing behavior as a function of r. We first tested whether this increasing behavior matches the expectation from perturbation theory. Neglecting logarithmic corrections we fitted the data at $r/a \in [2, 5]$ to

$$V^{(1)}_{\text{fit-1}}(r) = -\frac{c'}{r^2} + \mu' \,, \tag{6}$$

and found $c' = 0.099(5)$ and $a^2\mu' = 0.401(1)$ with $\chi^2_{\rm min}/N_{\rm df} = 6.6$, where the fit curve is plotted in Fig. 3 (dashed line). Note that if we include the data at $r/a = 6$, χ^2 becomes twice as large, while the fit parameters are little affected. In order to check if this is a remnant of the perturbative behavior, we need data at smaller distances and perform a scaling test. At the moment, what we can say is that the data at $r/a \gtrsim 5$ are inconsistent with a pure $1/r^2$ behavior.

In trying to establish empirically the functional form of the r dependence, we employed several alternative fit

functions, and among them, we found that

$$V^{(1)}_{\text{fit-2}}(r) = -\frac{c''}{r} + \mu'' \,, \tag{7}$$

can describe the behavior of $V^{(1)}(r)$ reasonably well, where the coefficient c'' has a dimension of mass. We took into account the data at $r/a \in [2,6]$ and obtained $ac'' = 0.081(4)$ and $a^2\mu'' = 0.417(1)$ with $\chi^2_{\text{min}}/N_{\text{df}} = 2.3$, where the fit curve is plotted in Fig. 3 (solid line).

As the potential $V^{(1)}(r)$ requires no matching coefficient [24, 25], in contrast to the spin-dependent potentials at $O(1/m^2)$, we can directly insert $V^{(1)}(r)$ into Eq. (1) and compare its relative magnitude with the static potential $V^{(0)}(r)$ for given quark and antiquark masses. For this purpose we may use the fit result of Eq. (7). By dividing $V^{(1)}_{\text{fit-2}}(r)$ by the quark mass, where we set $m_1 = m_2 = m$ for simplicity, we have a $1/r$ term with a dimensionless coefficient $2c''/m$. For charmonium, $m_c = 1.3$ GeV, we then find $2c''/m_c = 0.26(1)$, which is 93(5) % of the Coulombic coefficient of the static potential, $c = 0.281(5)$, in Eq. (2) [19]. For bottomonium, $m_b = 4.7$ GeV, we find $2c''/m_b = 0.073(4)$, which is still 26(2) % of c. It is certainly interesting to investigate the effect on heavy quarkonium spectroscopy.

IV. SUMMARY

We have investigated the relativistic correction to the static potential at $O(1/m)$ nonperturbatively by using lattice QCD Monte Carlo simulations for the first time. The key strategy here is to employ the multi-level algorithm for measuring the field strength correlator on the PLCF and to extract the potential by exploiting the spectral representation of the field strength correlators. This method allows us to obtain the potential with less statistical and systematic errors. The correction is found to be comparable to the Coulombic term of the static potential when applied to charmonium and to be one-fourth of the Coulombic term for bottomonium.

Finally, we note that the field strength correlator obtained here can be used to compute one of the velocity-dependent potentials at $O(1/m^2)$, $V_d(r)$, in the parametrization of Refs. [14, 15], since the spectral representation of $V_d(r)$ consists of the same amplitudes and the energy gaps. We plan to present this result as well as the other velocity-dependent potentials at $O(1/m^2)$ in a separate publication. The first lattice result can be found in Ref. [26].

Acknowledgments

We thank R. Sommer, N. Brambilla, A. Vairo and G.S. Bali for useful discussions. The main calculation has been performed on the NEC SX5 at Research Center for Nuclear Physics (RCNP), Osaka University, Japan. We thank H. Togawa and A. Hosaka for technical support.

[1] W. Lucha, F. F. Schöberl, and D. Gromes, Phys. Rept. **200**, 127 (1991).
[2] W. Buchmüller (Ed.), *Quarkonia*, Current physics-sources and comments, vol. 9, (North-Holland, 1992).
[3] G. S. Bali, Phys. Rept. **343**, 1 (2001), hep-ph/0001312.
[4] N. Brambilla *et al.*, *Heavy quarkonium physics*, CERN Yellow Report (2005), hep-ph/0412158.
[5] W. E. Caswell and G. P. Lepage, Phys. Lett. **B167**, 437 (1986).
[6] G. T. Bodwin, E. Braaten, and G. P. Lepage, Phys. Rev. **D51**, 1125 (1995), hep-ph/9407339, Erratum-*ibid* **D55**, 5853 (1997).
[7] N. Brambilla, A. Pineda, J. Soto, and A. Vairo, Nucl. Phys. **B566**, 275 (2000), hep-ph/9907240.
[8] N. Brambilla, A. Pineda, J. Soto, and A. Vairo, Phys. Rev. **D63**, 014023 (2001), hep-ph/0002250.
[9] A. Pineda and A. Vairo, Phys. Rev. **D63**, 054007 (2001), hep-ph/0009145, Erratum-*ibid* **D64**, 039902 (2001).
[10] N. Brambilla, A. Pineda, J. Soto, and A. Vairo, Rev. Mod. Phys. **77**, 1423 (2005), hep-ph/0410047.
[11] E. Eichten and F. Feinberg, Phys. Rev. Lett. **43**, 1205 (1979).
[12] E. Eichten and F. Feinberg, Phys. Rev. **D23**, 2724 (1981).
[13] D. Gromes, Z. Phys. **C22**, 265 (1984).
[14] A. Barchielli, E. Montaldi, and G. M. Prosperi, Nucl. Phys. **B296**, 625 (1988), Erratum-*ibid* **B303**, 752 (1988).
[15] A. Barchielli, N. Brambilla, and G. M. Prosperi, Nuovo Cim. **A103**, 59 (1990).
[16] K. Melnikov and A. Yelkhovsky, Nucl. Phys. **B528**, 59 (1998), hep-ph/9802379.
[17] A. H. Hoang, Phys. Rev. **D59**, 014039 (1999), hep-ph/9803454.
[18] N. Brambilla, A. Pineda, J. Soto, and A. Vairo, Phys. Lett. **B470**, 215 (1999), hep-ph/9910238.
[19] Y. Koma and M. Koma, "Spin-Dependent Potentials from Lattice QCD" (to be published).
[20] M. Lüscher and P. Weisz, JHEP **09**, 010 (2001), hep-lat/0108014.
[21] M. Koma, Y. Koma, and H. Wittig, PoS **LAT2005**, 216 (2005), hep-lat/0510059.
[22] Y. Koma, M. Koma, and P. Majumdar, Nucl. Phys. **B692**, 209 (2004), hep-lat/0311016.
[23] A. Huntley and C. Michael, Nucl. Phys. **B286**, 211 (1987).
[24] M. E. Luke and A. V. Manohar, Phys. Lett. **B286**, 348 (1992), hep-ph/9205228.
[25] A. V. Manohar, Phys. Rev. **D56**, 230 (1997), hep-ph/9701294.
[26] G. S. Bali, K. Schilling, and A. Wachter, Phys. Rev. **D56**, 2566 (1997), hep-lat/9703019.
[27] M. Lüscher, K. Symanzik, and P. Weisz, Nucl. Phys.

B173, 365 (1980).
[28] M. Lüscher, Nucl. Phys. **B180**, 317 (1981).
[29] One may assume the Lüscher term $c = \pi/12 \approx 0.262$ at long distances [27, 28].
[30] In practice, however, the integration of the field strength correlator on the lattice and the extrapolation of the temporal size of the Wilson loop to infinity cause systematic errors, which must be evaluated carefully.